Finger-jointed wood compressed parallel to the grain: experiment and modelling

Timmo Gavrilov*, and *Gennady* Kolesnikov

Petrozavodsk State University, Lenin Str., 33, 185910, Petrozavodsk, Russia

Abstract. Compression tests of pine specimens of two types with initial dimensions of 40x40x80 mm and 40x40x80 mm with finger-joints are considered. Tests on similar specimens without finger-joints are also analyses for comparison. The experiments showed that the finger-joint in the investigated specimens reduced the peak load on the specimen as well as the load in the post-peak stage of plastic deformation. A methodology for modelling the load-displacement relationship taking into account the plastic deformation of wood with a finger-joint in the post-peak stage is proposed. The modelling results do not contradict the experimental data. The basic equation of the proposed mathematical model can be used in further studies to analyse the energy characteristics of the deformation process of wooden elements of building structures.

1 Introduction

The use of wood in construction and other applications fulfils the criteria for sustainable development, one of which is the rational use of resources and the reduction of production waste [1, 2]. The development of this direction is promoted by the technology of finger adhesive joints, for example, in accordance with GOST 19414-2023. The GOST uses the term "finger adhesive joints", similar to the term in the English-language literature [3-5]. This technology makes it possible to obtain thin, almost endless blanks from small pieces of wood [3, 4]. This method minimizes the amount of wood waste and ensures sustainable wood management. For example, according to the study of [5], a multi-objective modified "firefly algorithm" determines the finger-joint parameters that maximise joint strength while reducing waste in the production of wooden structures.

However, issues related to modelling the behaviour of wood under load remain relevant [6]. One of such issues is a detailed description of the condition of finger-joints in wooden structures under compression, bending and tension. In this direction, an important study is [7], in which the authors used the finite element method to determine areas of stress concentration, i.e. potential localisation of wood damage in the finger-joint zone.

This paper is devoted to the analysis of the behaviour of finger-joints of wooden structures under compression parallel to the grain. Experimental methods and mathematical modelling methods were used as research tools. In this paper, the mathematical description

* Corresponding author: gtimmo@mail.ru

of the behaviour of specimens with finger-joints is based on the adaptation of previously derived equations [8, 9] to solve a new problem.

2 Methodology and Results

2.1 Experiment

The purpose of the experiment was to plot the force-displacement relationship for pine samples without joints and with finger-joints. A Shimadzu testing machine provided the experimental part of the study (fig. 1).

Fig. 1. Testing machine.

Figure 2 shows pine specimens in the form of a cube with initial dimensions of 40x40x40 mm, without finger-joints, before and after compression.

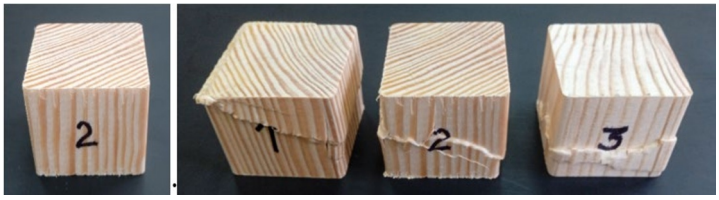

Fig. 2. Specimens without finger-joints before and after loading.

Figure 3 shows the load-displacement plot for the Figure 2 specimens at a controlled displacement rate of 10 mm/min. The average values of force and displacement at the peak are 84.171 kN and 1.382 mm, respectively.

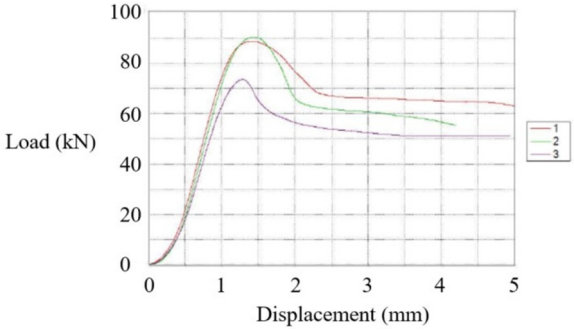

Fig. 3. Experimental load-displacement curves for the samples by Figure 2.

Figure 4 shows cube-shaped pine specimens with initial dimensions of 40x40x40 mm, with finger-joints, before and after testing.

Fig. 4. Specimens with finger-joints before and after testing.

Figure 5 shows the load-displacement curves for the Figure 4 specimens under controlled displacement at a rate of 10 mm/min. The average force and displacement values at the peak are 77.592 kN and 1.177 mm, respectively.

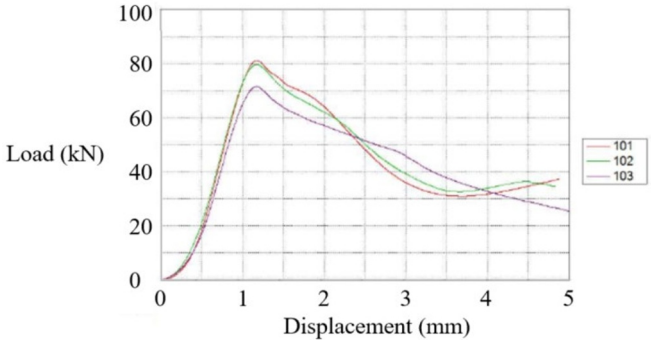

Fig. 5. Experimental load-displacement curves for specimens by Figure 4.

A comparison of Figures 2 and 4 shows that finger-joints localize wood damage i.e. are damage attractors. This picture of destruction is consistent with the numerical study cited above [7], which determined an increase in stress in the area of finger-joints, and, consequently, local destruction of wood in such a joint.

Comparison of the curves in Figures 3 and 5 shows that the finger-joint reduces the average force at peak from 84.171 to 77.592 kN, the average displacement at the same point from 1.382 to 1.177 mm, and the plastic stage transition load from about 60 kN to 30 kN.

Figure 6 shows pine specimens with initial dimensions of 40x40x80 mm, without finger-joints, before and after testing.

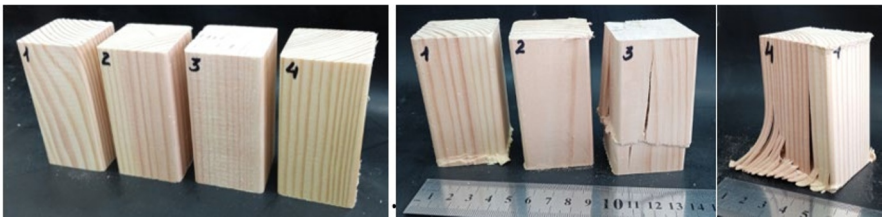

Fig. 6. Specimens with finger-joints before and after testing.

Figure 7 shows the load-displacement curves for the Figure 6 specimens under controlled displacement at a rate of 5 mm/min. The average force and displacement values at the peak are 73.9 kN and 1.484 mm, respectively.

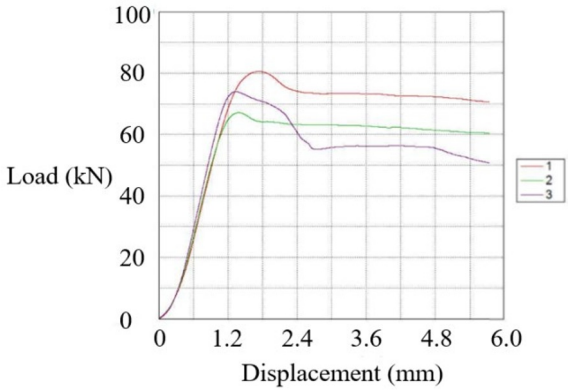

Fig. 7. Experimental load-displacement curves for specimens by Figure 6.

Figure 8 shows pine specimens with initial dimensions of 40x40x80 mm.

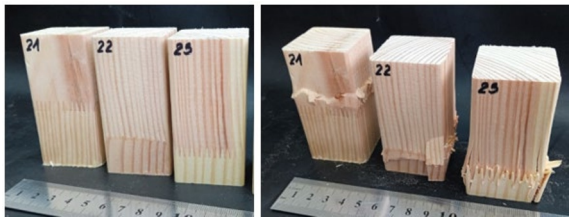

Fig. 8. Specimens with finger-joints before and after compression.

Figure 8 shows that finger-joints localize wood damage i.e. are damage attractors. This pattern of destruction is consistent with the numerical study cited above [7], which determined an increase in stress in the area of finger-joints, and, consequently, local destruction of wood in such a joint.

Figure 9 below shows the load-displacement curves for the Figure 8 specimens under controlled displacement at a rate of 5 mm/min. The average values of force and displacement at the peak point are 65.816 kN and 1.155 mm, respectively. The decrease in the average peak load value compared to specimens of the same cross section (Figure 2 and 3) from 84.171 to 65.816 kN is attributed to the effect of strain rate, namely, as experimentally shown in [10], the compressive strength of wood decreases with decreasing strain rate.

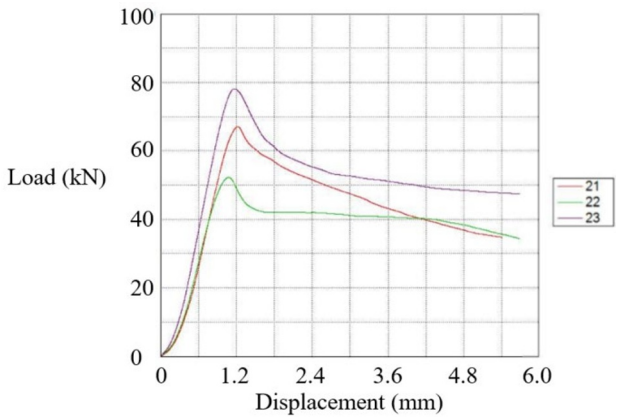

Fig. 9. Experimental load-displacement curves for specimens by Figure 8.

A comparison of Figures 7 and 9 shows that the gear connection reduces the average load and displacement values at the peak point as well as the load in the post-peak plastic deformation stage, i.e., the trend noted above when comparing the curves from Figures 3 and 5.

2.2 Modelling

The experimental load-displacement plots for wood compression presented above include an ascending branch, a peak point and a descending branch (Figures 3, 5, 7, 9). The behavior of wood before and after the peak point is significantly different, so some models contain two or more equations for the pre-peak and post-peak branches of the load-displacement (or stress-strain) curves, as discussed in [6].

To reduce the number of equations used, this paper proposes a different approach: the same equation describes both left and right branches, but with different parameter values. This approach to modelling timber structural elements requires only one additional equation that models the transition of wood into the plastic stage of deformation. Geometrically, this additional equation defines a line segment parallel to the horizontal axis (i.e., the displacement axis) and passing through the inflection point on the downward branch of the full load-displacement curve. The equation $\frac{d^2F}{du^2} = 0$ determines the abscissa of the inflection point. The function $F = F(u)$ has the following form [8]:

$$\frac{F}{F_{peak}} = \left(\frac{u}{u_{peak}} e^{\frac{1}{n}\left(1 - \frac{u^n}{u_{peak}^n}\right)} \right)^B . \quad (1)$$

The parameters n and B are determined during model calibration, similar to [11], e.g., using the least squares method. However, given the nonlinear nature of dependence (1), it is easier to apply the random search method [12].

For the left branch $0 \le u \le u_{peak}$; $n = n_l$; $B = B_l$.

For the right branch $u_{peak} \le u$; $n = n_r$; $B = B_r$.

For example, for sample 23 in Figure 8, the experimental curve shows Figure 9. Applying equation (1), we find: $n_l = 6.617$; $B_l = 1.450$; $n_r = 1.499$; $B_r = 1.075$. In Figure 10, the solid line is plotted using equation (1). Experimental data for sample 23 (Figure 8) are indicated by circles. Green circles indicate inflection points.

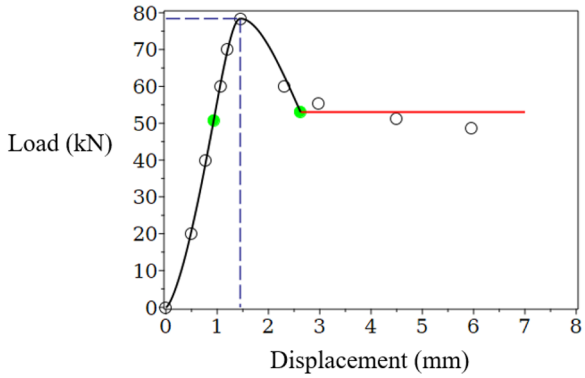

Fig. 10. Load-displacement plot considering the transition to the plastic deformation stage (red line).

3 Discussion

Of practical and scientific interest, is a more complete answer to the question: why does a fracture occur in the finger-joint zone? A reasonably complete answer touches on many aspects beyond the boundaries of this paper. In addition to the stress concentration studied in [7], we note that the strength, stiffness and other properties of wood vary greatly depending on the conditions of origin [6]. Therefore, in the region of the adhesive finger-joint, the strength and stiffness of one part of the specimen is likely to be different from the strength and stiffness of the other part. A stiffer and stronger material causes buckling of a less stiff and rigid material. The process is similar to dosed-load hardness testing such as Brinell or Rockwell. In our tests of a wooden specimen, the testing machine generated a load that induced deformation of the specimen, including a transition into the plastic deformation stage before the specimen was completely damaged.

In addition, despite the consistency of the results presented with experiments and previous work [13], further research on this topic is advisable, as the number of samples studied is small. From a practical point of view, the results of research in the affected area can contribute to the implementation of specific projects in accordance with sustainable development criteria [14–20].

4 Conclusion

Compression tests of pine specimens of two types with initial dimensions of 40x40x80 mm and 40x40x80 mm with finger-joints are considered. Tests on similar specimens without joints are also analyses for comparison. Experiments showed that the finger-joint in the studied specimens reduced the peak load on the specimen as well as the load in the post-peak stage of plastic deformation.

This paper proposes a methodology for modelling the load-displacement relationship considering the plastic deformation of timber with a finger-joint at the post-peak stage. The modelling results do not contradict the experimental data. The basic equation of the mathematical model (1) can be useful in further research to analysis the energy characteristics of the deformation process of wooden elements in the interests of sustainable development.

Despite the consistency of the presented experimental and modelling data, further research on this topic is advisable, as the number of samples studied is small.

References

1. F. Arriaga, X. Wang, G. Íñiguez-González, D.F. Llana, M. Esteban, P. Niemz, Forests, **14**, 1202 (2023) https://doi.org/10.3390/f14061202
2. R. Sikkema, D. Styles, R. Jonsson, B. Tobin, K.A. Byrne, Sustainable Cities and Society, **90**, 104370 (2023) https://doi.org/10.1016/j.scs.2022.104370
3. C.K. Muthumala, S. De Silva, K.K.I.U. Arunakumara, P. L. A. G. Alwis, J. Fail. Anal. Prev. **21**, 2215–2223 (2021). https://doi.org/10.1007/s11668-021-01274-9
4. J. Hou, A. Taoum, N. Kotlarewski, G. Nolan, Forests, **14**, 1192 (2023) https://doi.org/10.3390/f14061192
5. S.T. Le, T.N. Nguyen, D.-K. Bui, Q.P. Ha, T.D. Ngo, Buildings, **13**, 1186 (2023) https://doi.org/10.3390/buildings13051186
6. S.M. Walley, S.J. Rogers, Materials, **15**, 5403 (2022) https://doi.org/10.3390/ma15155403
7. A. Vega, V. Baño, A. Cardoso, L. Moya, Eur. J. Wood Prod. **78**, 923–932 (2020). https://doi.org/10.1007/s00107-020-01570-5
8. V. Shekov, G. Kolesnikov, Materials, **16**, 4875 (2023) https://doi.org/10.3390/ma16134875
9. G. Kolesnikov, V. Shekov, Materials **15**, 7907 (2022) https://doi.org/10.3390/ma15227907
10. Dobrowolska, E., Lichaczewska, B., O. Pinchevska, *Annals of Warsaw University of Life Sciences-SGGW. Forestry and Wood Technology*, **109**, 126-136 (2020) https://bibliotekanauki.pl/articles/2200230.pdf
11. N. Stojković, D. Perić, D. Stojić, N. Marković, Teh. Vjesn. **24**, 863 (2017) DOI: 10.17559/TV-20151027225413
12. J.S. Arora, O.A. Elwakeil, A.I. Chahande, C.C. Hsieh. Structural Optimization, **9**, 137–159 (1995). https://doi.org/10.1007/BF01743964
13. G. Kolesnikov, T. Gavrilov, M. Zaitseva, Symmetry, **15(2)**, 274 (2023) https://doi.org/10.3390/sym15020274
14. A. Kuzmenkov, E3S Web of Conferences, **458**, 07006 (2023) https://doi.org/10.1051/e3sconf/202345807006
15. S. Buryachenko, Z. Voronin, I. Karachentseva, A. Kuzmenkov, O. Popova, E3S Web of Conferences 263, 05018 (2021) https://doi.org/10.1051/e3sconf/202126305018
16. A. Kuzmenkov, I. Karachentseva, E3S Web of Conferences 402, 07001 (2023) https://doi.org/10.1051/e3sconf/202340207001
17. M.R. Cabral, P. Blanchet, Buildings, **14(1)**, 63 (2024) https://doi.org/10.3390/buildings14010063
18. M.R. Cabral, P. Blanchet, Materials, **14**, 1848 (2021) https://doi.org/10.3390/ma14081848
19. R. Husgafvel, D. Sakaguchi, Sustainability, **15**, 7871 (2023) https://doi.org/10.3390/su15107871
20. N. Gutiérrez, J. Negrão, A. Dias, P. Guindos, Sustainability, **16**, 2134 (2024) https://doi.org/10.3390/su16052134
21. L.A. Rocha, R.S. Gomez, J.M.P.Q. Delgado, A.N.O. Vieira, I.B. Santos, M.R. Luiz, V.A.B. Oliveira, G.L. Oliveira Neto, D.B.T. Vasconcelos, M.J.V. Silva et al., Buildings, 13, 1408 (2023) https://doi.org/10.3390/buildings13061408